Neutron Reflectometry Using the Kinematic Approximation and Surface Quasi-Elastic Light Scattering from Spread Films of Poly(methyl methacrylate)

J. A. Henderson and R. W. Richards*

Department of Chemistry, University of Durham, Durham DH1 3LE, U.K.

J. Penfold

ISIS Science Division, Rutherford-Appleton Laboratories, Chilton, Didcot OX11 0QE, U.K.

R. K. Thomas

Physical Chemistry Laboratory, University of Oxford, Oxford OX1 3QZ, U.K.

Received May 15, 1992; Revised Manuscript Received September 22, 1992

ABSTRACT: Neutron reflectometry data for syndiotactic poly(methyl methacrylate) have been analyzed using the kinematic approximation. This has produced form factor and Guinier analyses of the data from which the thickness and composition of films spread at the air–water interface have been determined. The layer thickness remains remarkably constant at ca. 18 (±2) Å over a surface concentration ranging from 0.2 to 2.0 mg m^{-2}. Water is always contained in the film at a very small volume fraction (≈0.1), the polymer volume fraction increases linearly with surface concentration up to ca. 1.5 mg m^{-2}; thereafter the volume fraction of polymer is approximately constant at 0.9 for the higher surface concentrations in the range investigated. Surface quasi-elastic light scattering has been used to evaluate the surface viscoelastic parameters of the polymer film. The dilational modulus (ϵ_0) obtained from surface quasi-elastic light scattering has the same general features as that obtained from surface pressure data but is shifted to a lower concentration. There is evidence from the surface tensions obtained that there is anomalous behavior at low values of the surface concentration of polymer. Over the range of surface concentrations investigated, the loss modulus of the polymer film decreases linearly with the reciprocal of the polymer content of the film.

Introduction

Spread films of polymers at the air–water interface are of both scientific and technical interest. They may be utilized as simple models for membranes, and they constitute a situation wherein polymer molecules are pseudo-two-dimensional. There have been many studies of the surface pressure–area isotherms of a variety of polymers; in the past the interpretation of the isotherms had been qualitative.[1-4] Recently there have been more quantitative discussions of surface pressure isotherms of polymers.[5-10] Application of scaling laws to spread polymer films has enabled a more quantitative discussion of the isotherms, and excellent discussions of the use of these ideas have been provided in the work of Kawaguchi et al.[7,8] and Rodelez et al.[9] Evidence that crystallization takes place within a spread film of isotactic poly(methyl methacrylate) when compressed has been concluded by Brinkhuis and Schouten[10] from surface pressure isotherms and grazing incidence reflection IR studies. However, since the spatial resolution of this latter technique is on the order of microns, whereas the thickness of the spread films is on the order of 10 Å, explicit conclusions about the compositional uniformity of the surface film normal to the air–water interface cannot be made.

Neutron reflectometry[11] (NR) and surface quasi-elastic light scattering[12] (SQELS) are techniques which can provide information on the structure (normal to the interface) and viscoelastic properties of spread films. Both have been extensively applied to surfactants and spread films[13-15] of low molecular weight materials, but there has been little discussion of their use in the investigation of spread films of synthetic polymers. In an earlier paper[16] we reported NR measurements on tactic isomers of poly(methyl methacrylate) (PMMA), where the data were analyzed by optical matrix methods. This analysis showed that the surface films had a thickness of ca. 18 Å over a surface concentration (Γ_s) range of 0.1–2.0 mg m^{-2} and that they contained an almost constant volume fraction of water with an air content that decreased as Γ_s increased. The most detailed application of SQELS to PMMA surface films has been that of Yu et al.[17] although Langevin[18] reported some early results. In the analysis of their data, Yu et al. assumed that the transverse shear viscosity is zero, an assumption that has been demonstrated to be invalid.[19] Furthermore, the parameters they extracted from their data were subjected to considerable error due, in part, to the very "stiff" nature of PMMA surface films. The analysis of both NR and SQELS data has been considerably improved since the results referred to above were obtained. First, in NR, Thomas et al.[20] have used the kinematic approximation to analyze weak specular reflection data; this approach requires no assumptions about the distribution of matter at the air–water interface. Second, Earnshaw[21,22] has demonstrated that the use of heterodyne detection, with photon correlation spectroscopy, and a direct analysis of the data so obtained can be extremely successful in extracting the four surface viscoelastic parameters of a surface film from SQELS data.

We report here the application of formulas derived from the kinematic approximation to neutron reflectometry data for syndiotactic PMMA and the dependence of surface viscoelastic parameters obtained by SQELS on the surface concentration of PMMA. The latter data are confined to one incident **Q** vector only, and therefore we do not report on the frequency dependence of the surface viscoelastic properties; nevertheless, an insight into the surface concentration dependence of these properties is provided. Using the kinematic approximation and the newly developed partial structure approach to the analysis of

* To whom correspondence should be addressed.

0024-9297/93/2226-0065$04.00/0

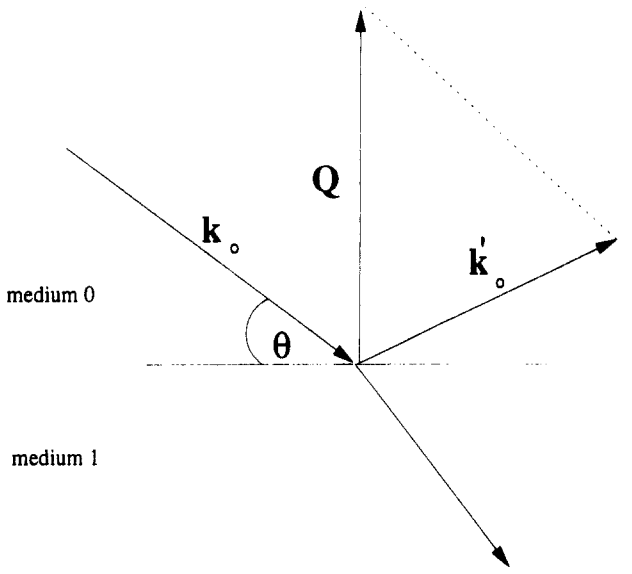

Figure 1. Wave vectors and the scattering vector defined for a neutron beam incident at an angle of θ with the interface between mediums 0 and 1.

neutron reflectometry data, it is possible to make some deductions regarding the uniformity of the surface layers within the minimum distance scale probed by the neutron beam. We give below the essential equations of the kinematic approximation for neutron reflection and a précis of the underlying theory of SQELS.

Theoretical Background

Neutron Reflectometry. The basic theory and underlying principles of neutron reflectometry have been detailed in several publications, and an outline was provided by us in an earlier publication.[16] To date, much of the analysis has used variations of the optical matrix method. This approach requires the assumption of a model and the fitting of this model to the data by adjusting such parameters as the scattering length density[23] and thickness of the surface layer or layers. Apart from the correctness of the model, there is always concern about the uniqueness of the fit to the data, and a rigorous search for the true minimum in the surface of the "goodness of fit" criterion must be made. The use of contrast variation can help in this model fitting since specific labeling of parts of the system can aid the identification of the various contributions to the reflection profile. By applying the kinematic approximation to specular reflectivities with a magnitude of much less than 1, Thomas et al.[20] have shown that the assumption of a model can be dispensed with and that, by exploiting to the fullest the contrast variation possible by replacing hydrogen atoms in the system with deuterium, a unique description of the surface layer can often be obtained.

The aim of neutron reflectivity is to obtain the distribution of scattering length density, $\rho(z)$, normal to the surface plane located at $z = 0$. Variations in the plane are ignored; i.e., the surface is smooth with respect to the wave vectors probed by the incident neutron beam. We consider the situation shown in Figure 1, a plane wave of neutrons is incident on the surface of medium 1 at a glancing angle of θ. The incident and scattered wave vectors are k_0 and k'_0, and the scattering vector $\mathbf{Q} = (k'_0 - k_0)$. Since the two wave vectors have equal magnitudes ($2\pi/\lambda$), then $|\mathbf{Q}| = Q = (4\pi/\lambda) \sin\theta$. In the kinematic approximation[13,20] the specular reflectivity is related to the one-dimensional Fourier transform of $\rho(z)$ by

$$R(Q) = (16\pi^2/Q^2)|\rho(Q)|^2 \tag{1}$$

This equation is valid for Q values much larger than the critical value (Q_c) below which total reflection takes place; in practice this means that the reflectivities must be less than 10^{-2}. For the situation where the media on either side of the surface film have identical scattering length densities, then the reflectivity can be written as

$$R(Q) = R_s^{\circ}(Q)\, h(Q) \tag{2}$$

with

$$R_s^{\circ}(Q) = (16\pi^2/Q^2)|m|^2$$

$$h(Q) = |\rho(Q)/\rho(0)|^2$$

$$m = \int_{-\infty}^{\infty} \rho(z)\, dz$$

where $h(Q)$ is the form factor, determined by the structure of the surface, and m is the surface excess scattering length density. For small values of scattering vector $\mathbf{Q}$ the form factor can be expressed in the Guinier approximation as

$$h(Q) = \exp(-Q^2\sigma^2) \tag{3}$$

with σ being the standard deviation of $\rho(z)$; thus

$$R(Q) = (16\pi^2/Q^2)|m|^2 \exp(-\sigma^2Q^2)$$

Hence

$$\ln (Q^2R(Q)) = \ln(16\pi^2|m|^2) - \sigma^2Q^2 \tag{4}$$

The situation with the media on each side of the interface being identical can be obtained by making the aqueous subphase, on which the polymer film is spread, a mixture of H_2O and D_2O such that the scattering length density is zero and equal to that of air; this is often referred to as air contrast matched water.

If the reflectivity is expressed in terms of the *gradient* of $\rho(z)$, $(d\rho(z)/dz)$, then

$$R(Q) = (16\pi^2/Q^4)|\rho'(Q)|^2 \tag{5}$$

where $\rho'(Q)$ is the one-dimensional Fourier transform of $d\rho(z)/dz$. Now consider the scattering length density profile shown in Figure 2a, which schematically is identical to an idealized surface film of hydrogenous PMMA spread on D_2O. The gradient in $\rho(z)$ is shown in Figure 2b and corresponds to two Δ functions at the interfaces of the polymer layer with air and the subphase, respectively. Now the Fourier transform of the Patterson function[24] of $(d\rho/dz)$ is $|\rho'(Q)|^2$, the form factor of the gradient in scattering length density, with the Patterson function, $P'(z)$, being the correlation function of the gradient in scattering length density defined by

$$P'(z) = \int_{-\infty}^{\infty} \rho'(z)\, \rho'(z-u)\, du \tag{6}$$

Figure 2c is the Patterson function obtained from Figure 2a and is three Δ functions located at $-d$, 0, and d from the surface, with the origin for d being located at the surface. The Fourier transform of this collection of Δ functions has been shown to be[20]

$$|\rho'(Q)|^2 = \Delta\rho^2 - 4\rho(\Delta\rho - \rho) \sin^2 (Qd/2)$$

and Figure 2d shows the schematic variation of the form factor, $|\rho'(Q)|^2$, with Q predicted by this equation, and for a uniform layer the deep minima occur at $Q = \pi/d, 3\pi/d,$

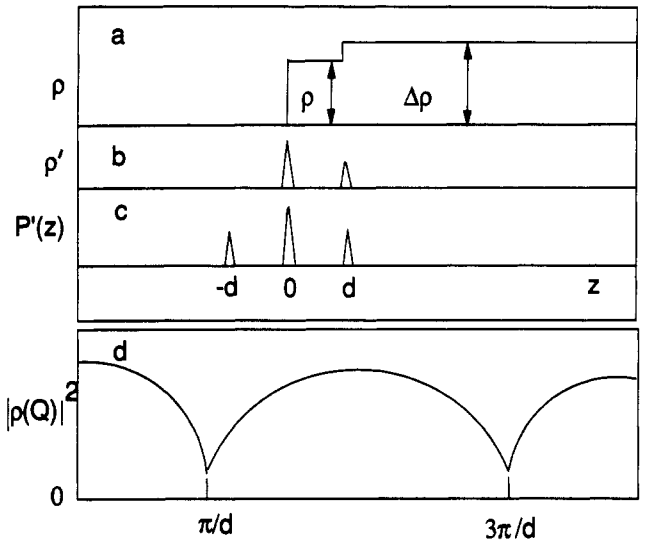

Figure 2. (a) Schematic scattering length density profile for hydrogenous PMMA on D_2O. (b) Gradient in the scattering length density profile. (c) Patterson Function. (d) Form factor $\equiv (Q^4/16\pi^2)R(Q)$.

etc., where d is the surface layer thickness. Experimentally, the form factor can be obtained by a rearrangement of eq 5 to

$$|\rho'(Q)|^2 = (Q^4/16\pi^2)R(Q) \tag{7}$$

Thus by manipulating the scattering length densities (and hence contrast) of the polymer and subphase, the reflectivities can be interpreted using eq 4 for air contrast match conditions; the scattering length density of the layer from the value of m can be obtained. Equation 7 can be used for any contrast between the subphase and upper medium to yield the layer thickness (or at least its uniform layer equivalent).

Surface Quasi-Elastic Light Scattering.[25,26] The surface of a liquid is macroscopically flat, but on a microscopic scale it is subject to continual roughening by thermal fluctuations which constitute the capillary waves on the surface. For water the amplitude of these waves is ca. 2 Å, and although small, they are responsible for the surface scattering of light. The amplitude of a capillary wave propagating in the x direction is $\zeta_0 \exp(i(Qx + \omega t))$, where the frequency, ω, controls the temporal evolution of the waves and is a complex quantity, $(\omega_0 + i\Gamma)$, with ω_0 being the capillary wave frequency and Γ the decay constant which determines the damping of the waves. The capillary waves have a spectrum of frequencies and wavelengths, the incident scattering vector, Q, probes capillary waves of wavelength λ such that $Q = (2\pi/\lambda)$, and the complex frequency of the waves is related to Q via a dispersion equation.[27] The dispersion equation depends not only on ω and Q but also on the density, viscosity, surface tension, γ, and dilational modulus, ϵ, of the liquid surface. Strictly, the dilational modulus arises from the compression (longitudinal modes) of a surface film, and such fluctuations scatter light but weakly; however, they are coupled with the transverse modes (capillary waves) whose amplitude is chiefly controlled by γ. Since energy may be dissipated in the surface film, both γ and ϵ are strictly viscoelastic quantities with

$$\gamma = \gamma_0 + i\omega\gamma' \tag{8}$$

$$\epsilon = \epsilon_0 + i\omega\epsilon' \tag{9}$$

In eqs 8 and 9, γ_0 is the classical surface tension and ϵ_0 the dilational modulus, which classically is defined by $\Gamma_s(d\pi/d\Gamma_s)$, π being the surface pressure exhibited by a surface film of concentration Γ_s. The corresponding shear viscosity, γ', and dilational viscosity, ϵ', are somewhat ill-defined, but they are not the commonly described classical viscosities.[28] The shear viscosity controls the response to a transverse shearing of the surface; the dilational viscosity influences the in-plane compression of the surface film.

Using the dispersion equation, the power spectrum of light scattered by the capillary waves can be calculated as a function of ω. Although this power spectrum can be, and has been, experimentally measured, a more rapid means of obtaining information on the viscoelastic properties of a surface layer is by photon-correlation spectroscopy. The correlation function is simply the Fourier transform of the power spectrum. Although the capillary waves are efficient scatterers of light, the intensity of scattering is weak, and hence, to improve the quality of the data, it is normal to use heterodyne detection where the scattered light is mixed with a reference beam of light. Details of the technique and complete expositions of the theory have been given by several workers,[26,30] notably by Earnshaw.[25,29]

There has been little work done on polymers spread at the air–water interface. What has been done has usually extracted information by solving the dispersion equation by presuming γ' is zero. This last assumption is by no means valid. A much more powerful and unambiguous analysis of the quasi-elastic light scattering data has been developed by Earnshaw[19,22] which enables the extraction of all the parameters (γ_0, ϵ_0, γ', and ϵ') from the heterodyne correlation function. The justification of this approach and experimental demonstrations of its correctness have been discussed at length and are so convincing that it is this direct analysis we have used here.

Table I
Molecular Weight and Tacticity of Syndiotactic Poly(methyl methacrylate)

	$M_w/10^3$	$M_n/10^3$	fraction of racemic groups	fraction of meso groups
hydrogenous	267.0	119.0	0.85	0.15
deuterated	335.0	151.0	0.87	0.13

Experimental Section

Materials. Syndiotactic poly(methyl methacrylate) (synPMMA), both hydrogenous and deuterated, was prepared by anionic polymerization of purified monomers under high vacuum at 195 K in tetrahydrofuran using 9-fluorenyllithium as the initiator. After isolation and drying, each polymer was analyzed by size-exclusion chromatography, using a combined refractometric and viscosity detector (Viscotek), and ^{13}C NMR (400-MHz proton frequency). The results of these analyses are given in Table I.

Surface Pressure Isotherms. The details of the determination of the surface pressure isotherms have been given earlier.[16] In brief, the synPMMA was spread from chloroform solution onto the surface of electrochemical purity water contained in a surface film balance (NIMA Technology, Warwick, England). The spread layer was then compressed at a constant rate of 30 cm^2 and the surface pressure recorded continuously on a computer. These data were used to define the surface concentrations for the neutron reflectometry data since the surface pressure was not recorded simultaneously during these latter experiments. SQELS measurements were made using the same Langmuir trough as for the surface pressure measurements, and consequently the static surface pres-

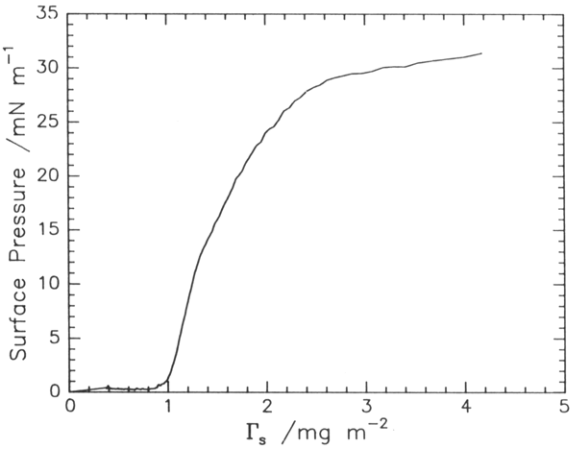

Figure 3. Typical surface pressure isotherm obtained for SynPMMA spread at the air–water interface at 298 K.

sure was recorded at the same time as the SQELS data were collected. The nature and scaling exponents of the surface pressure isotherms have been thoroughly discussed in the earlier publication;[16] a typical surface pressure isotherm is given in Figure 3.

Neutron Reflectometry. The details of the neutron reflectometry experiments have been set out in an earlier publication,[16] but a précis will be given here. A Langmuir–Adams trough, milled from a solid block of poly(tetrafluoroethylene) (PTFE), was sealed from the atmosphere in an aluminum box with quartz inlet and outlet windows for the neutron beam. Adjustable barriers aligned parallel to the incident beam direction allowed compression of the polymer film in situ. The trough was mounted in the beam and aligned with the aid of a laser beam reflected from the liquid surface. A "monolayer" of PMMA was spread on the surface by dispensing a few microliters of a chloroform solution of PMMA onto the surface through a resealable hole in the aluminum box. Two differing contrast conditions were used; perdeuterated poly(methyl methacrylate) was spread on air contrast matched water and the hydrogenous polymer was spread on D_2O. The range of surface concentrations Γ_s used was from 0.2 to 2.0 mg m^{-2}. Restrictions in available beam time prevented us from collecting reflectometry data for the hydrogenous polymer spread on D_2O at Γ_s values of 0.3 and 0.5 mg m^{-2}.

All reflectometry experiments were made on the CRISP reflectometer on the ISIS pulsed neutron source located at the Rutherford–Appleton Laboratory. The data were obtained as reflectivity (plus errors) as a function of the scattering vector, Q, normal to the reflecting surface, and the range of scattering vector investigated was from 0.05 to 0.65 Å^{-1}. The incident white neutron beam has a wavelength range of 0.5 to 6.5 Å and is inclined at 1.5^0 to the horizontal. The specularly reflected beam was detected by a shielded ^{3}He detector; the resolution in Q was 6%.

Surface Quasi-Elastic Light Scattering. SQELS experiments were made on an apparatus constructed in this laboratory. It is essentially identical to equipment described by others elsewhere[24,29] in greater detail. Figure 4 shows the major components of the apparatus. The light source was a 10-mW vertically-polarized laser which was mounted, together with other optical components, on a triangular optical bench. After passing through lens L1, the light is split into several diffracted beams (of much lower intensity) by passage through the transmission grating, T. These diffracted beams are in the horizontal plane, and those on one side of the main beam are attenuated by the neutral density filter, F. After passing through the lens L2, all the light is "periscoped" by mirrors

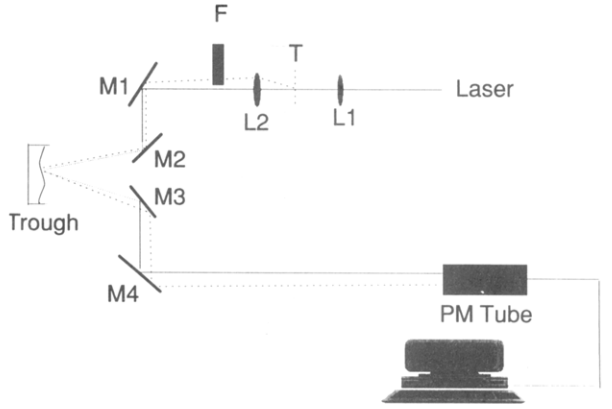

Figure 4. Sketch of SQELS apparatus.

M1 and M2 onto the liquid surface of the Langmuir trough. Lenses L1 and L2 focus the light onto the photomultiplier and image the grating T at the liquid surface. The scattered and reflected light is collected by mirror M3 and periscoped by mirror M4 onto the photomultiplier PM, all mounted on a second optical bench. The separate attenuated diffracted beams act as reference sources which beat with the scattered light at the photocathode of the photomultiplier. Each reference source is incident on the liquid surface at a different angle and thus probes a different wavelength ($\sim 2\pi/Q$) of the spectrum of capillary waves on the liquid surface and thus also probes a different capillary wave frequency. In the results reported here only one value of Q was used, 294 cm^{-1}. The heterodyne signal generated by the photomultiplier was collected by a Malvern K7025 correlator with 128 channels arranged serially. Control of the correlator was through a microcomputer which also stored each data set and transferred it to a micro-VAX 3100 for analysis. Both optical benches and the trough were placed on heavy optical tables which "floated" on nitrogen gas to reduce extraneous vibrations. The Q vector associated with each reference beam was calculated by noting the capillary wave frequency and damping constant obtained for highly purified water (Elgastat UHQ) using this apparatus together with literature values for the surface tension and viscosity of water and solving the dispersion equation.

Analysis of the SQELS data was a two-pass process. First, each data set was analyzed to obtain the frequency and damping constant of the capillary waves. These were obtained by a nonlinear least-squares fit of an expression for the correlation function which included corrections for the finite size of the laser beam and very long wavelength fluctuations ("droop") which are not removed by the optical table. Second, the surface tension, shear viscosity, dilational elastic modulus, and elastic viscosity were obtained by the direct procedure developed by Earnshaw et al.[19,22] In outline this consists of fitting the Fourier transform of the power spectrum obtained from the dispersion equation of the capillary waves. Strict boundary conditions are placed on the fitting parameters, the starting parameters of which are set when the analysis routine is begun. Both of these fitting procedures were provided by the kindness of Professor J. C. Earnshaw, Queen's University, Belfast, Ireland, and only trivially modified to suit local conditions.

Results

Neutron Reflectometry. A typical reflectometry profile is shown in Figure 5; evidently at Q values greater than 0.5 Å^{-1} the reflectivity has a constant value within the error. This constant value is due to the background

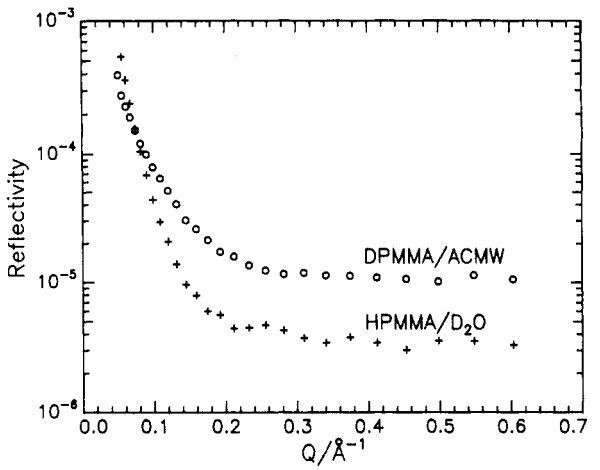

Figure 5. Neutron reflectivity profiles for syndiotactic poly(methyl methacrylate) (synPMMA) spread at the air–water interface. In each case the surface concentration of polymer is 1.0 mg m^{-2}. Error bars are within the size of the symbols.

from the instrument and the sample itself. It is also important to note that, even at the lowest value of Q investigated here, the reflectivity never exceeds a value of 10^{-3}. Furthermore, the critical value of $Q(Q_c)$, below which the total reflection is observed, for D_2O is 0.017 Å^{-1}; therefore, the conditions under which the kinematic approximation can be used prevail in the experiments reported here. Analysis via the kinematic approximation requires subtraction of the background which must be estimated accurately. Backgrounds were calculated from the observed reflectivity averaged over the last 6 points of each reflectivity profile. Experiments have shown that in this range of Q the resolution error has no influence on the background.[31] This value was subtracted from the data, and typical form factor plots which result are shown in Figure 6 for the hydrogenous polymer spread on D_2O. At high Q, the error bars become large due to the reflectivity approaching that of the background. Notwithstanding this, a sharp minimum is observed, as predicted by theory for a uniform layer. At the minimum where $Q = \pi/d$, then

$$Q^4R(Q) = 16\pi^2(2\rho_d - \Delta\rho)^2 \qquad (10)$$

with $\Delta\rho = \rho_{-\infty} - \rho_\infty$, i.e., the difference in scattering length densities of air and the subphase, respectively. Values of ρ_d, the scattering length density of the surface layer calculated from the minima, are quoted in Table II together with the thickness, d, of the synPMMA layer obtained.

Figure 7 shows the background subtracted data for the deuterated synPMMA spread on air contrast matched water plotted according to eq 4, a Guinier plot. The values of m and σ obtained from such plots are also given in Table II for all the values of Γ_s investigated. The effect of an increased surface concentration of polymer is clearly evident in the error bars since the signal to noise ratio increases at higher values of Γ_s.

Surface Quasi-Elastic Light Scattering. Typical intensity correlation functions are shown in Figure 8 for a low and a high value of Γ_s; data collection times were ca. 5 min in each case; for the lower value of Γ_s the signal to noise ratio is lower, and this becomes very evident at the longer delay times where the oscillations are almost completely damped out. Variation of the frequency, ω_0, and the damping constant, Γ, with surface concentration is shown in Figure 9. The vertical bars in Figure 9a,b indicate the magnitude of the errors in that region of surface concentration. The magnitude of the frequencies is of the same order as those reported by Kawaguchi et

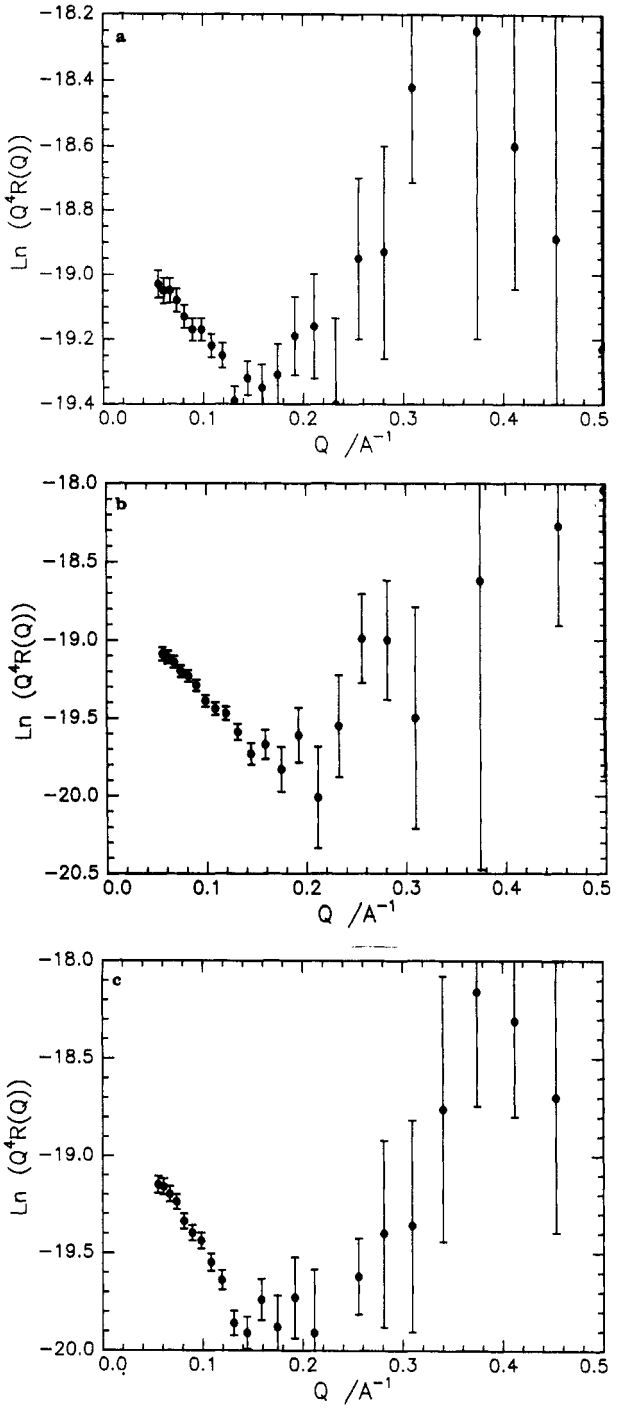

Figure 6. Form factors obtained for hydrogenous synPMMA spread on D_2O at three different values of surface concentration: (a) Γ_s = 0.4 mg m^{-2}; (b) Γ_s = 1.0 mg m^{-2}; (c) Γ_s = 2.0 mg m^{-2}.

al.,[17] but the dependence on Γ_s is completely different. Admittedly, our data do not extend to as low a value of Γ_s as those of Kawaguchi; however, we see little evidence of a plateau in capillary wave frequency at either low or high Γ_s values as reported by Kawaguchi et al. Similarly, the damping constants obtained by us show a steady decrease in value as Γ_s increases, whereas those reported by Kawaguchi et al. are sensibly constant until $\Gamma_s \approx 0.6$ mg m^{-2}, when a sudden increase by a factor of 2 to a higher plateau was recorded. Moreover, the damping factors obtained by us have a much smaller magnitude notwithstanding the error estimated from several repeated SQELS experiments at the same value of Γ_s. Each SQELS data set was analyzed by the direct analysis procedure outlined in the Experimental Section. The solid lines in Figure 8 are the resultant fits to the data which in all cases were

Table II
Primary Parameters Obtained from Patterson and Guinier Plots of Neutron Reflectometry Data

Γ_s/mg m^{-2}	$\rho_d{}^a$/10^{-6} Å^{-2}	d^b/Å	m^c/10^{-6} Å^{-1}	σ^d/Å	ρ_f/10^{-6} Å^{-2}
0.2	5.61	17.5			
0.3			19.8	6.1	
0.4	5.61	20.9	24.2	5.8	1.16
0.5			31.0	6.1	
0.6	5.49	20.9	37.9	4.2	1.81
0.8	5.38	19.6	65.7	5.6	3.35
1.0	5.17	18.5	76.3	5.8	4.12
1.5	5.17	17.5	103.0	6.9	5.88
2.0	5.07	17.5	108.3	7.5	6.19

[a] Error ±0.6 × 10^{-6} Å^{-2}. [b] Error ±2.0 Å. [c] Error ±0.5 × 10^{-6} Å^{-1}. [d] Error ±0.4 Å.

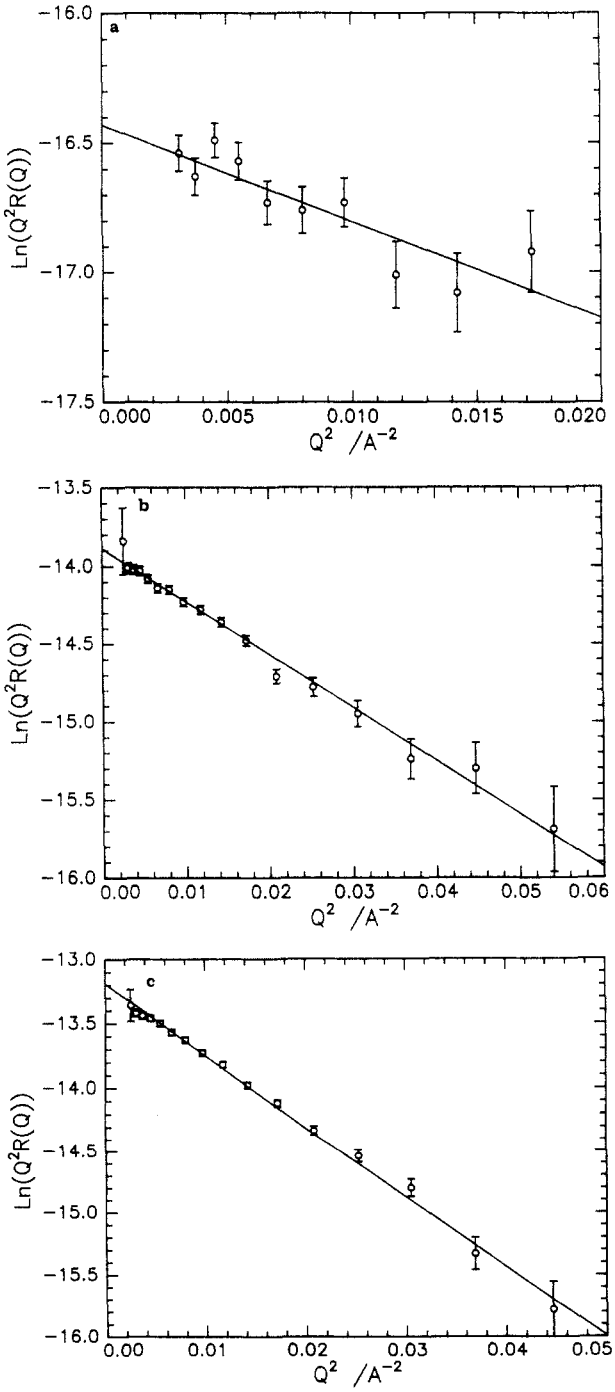

Figure 7. Guinier plots for deuterated synPMMA spread on air contrast matched water: (a) Γ_s = 0.4 mg m^{-2}; (b) Γ_s = 1.0 mg m^{-2}; (c) Γ_s = 2.0 mg m^{-2}.

of equal or better quality to those shown here. From these fits, values of γ_0, γ', ϵ_0, and ϵ' were obtained; however, the signal to noise ratios, particularly for the lower values of Γ_s, were such that the errors on ϵ' were very large, and hence the values of ϵ' were unreliable and are not discussed further here. By contrast the precision on γ_0 was on the order of ±0.05 mN m^{-1} at the very least, and the dependence of γ_0 on Γ_s is shown in Figure 10. Figures 11 and 12 show the dependence of the transverse shear viscosity, γ', and the dilational modulus, ϵ_0, as a function of Γ_s; both of these show a sharply defined peak at a finite value of Γ_s. The shear viscosity rapidly falls to zero after passing through a maximum, whereas the dilational modulus seems to display both a maximum and a minimum in its dependence on Γ_s.

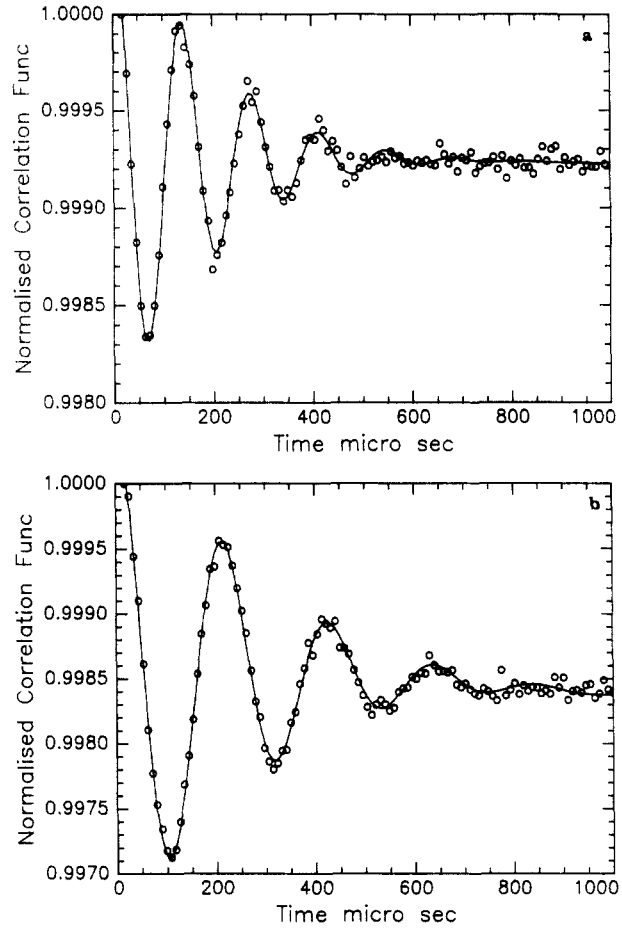

Figure 8. Normalized heterodyne correlation functions for synPMMA spread at the air–water interface: (a) Γ_s = 0.7 mg m^{-2}; (b) Γ_s = 1.75 mg m^{-2}. Solid lines are fits to the data using the direct analysis procedure.

Discussion

The values of the thickness of the surface layer of PMMA obtained using the Patterson analysis and set out in Table II are essentially constant over the whole range of Γ_s investigated and are broadly consistent with those obtained by the optical matrix methods. Values of the thickness obtained from the position of the minimum in the form factor plots of Figure 6 are not influenced by the magnitude of the background subtracted. Evidently, the magnitude of the background subtracted will have a severe influence on the value of ρ_d calculated from the ordinate value of the minimum; however, the asymptotic level at high Q values shown in Figure 5 is sufficiently constant over a large range of Q that we can be reasonably confident that the correct background has been subtracted. The quantity m obtained from the Guinier plots is the surface excess scattering length density, $\rho_s(z)$, integrated over the distance $-\infty \leq z \leq \infty$. The form factor plots of the data shown in

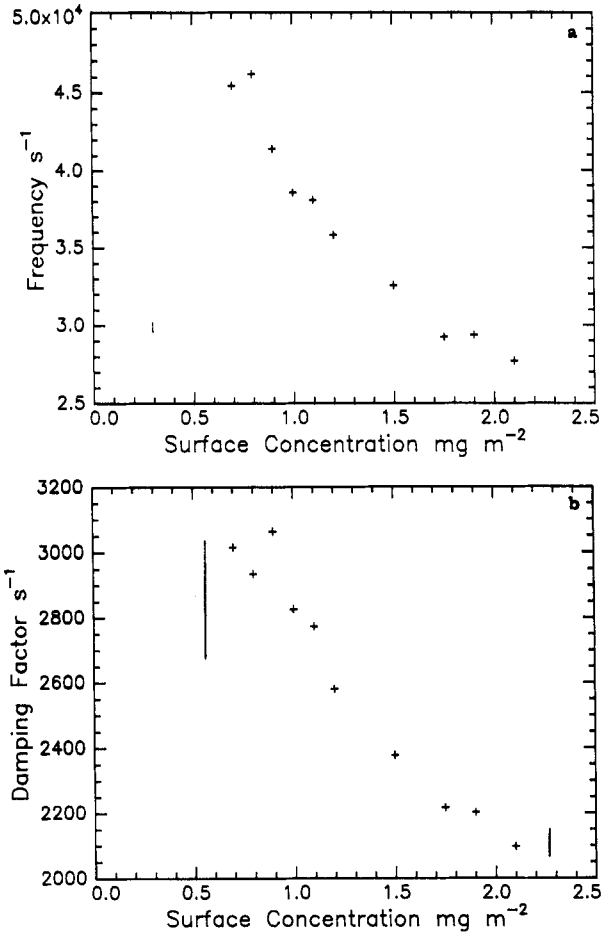

Figure 9. Primary parameters obtained by SQELS for synPMMA spread at the air–water interface. Vertical lines indicate the magnitude of the errors. (a) Dependence of the capillary wave frequency on surface concentration. (b) Dependence of the damping factor on surface concentration.

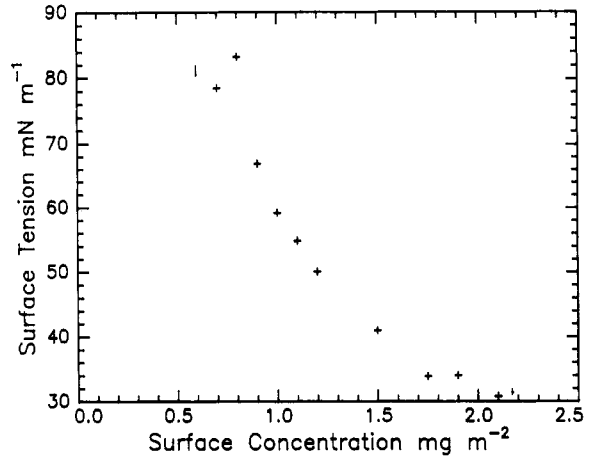

Figure 10. Surface tension evaluated by SQELS for synPMMA spread at the air–water interface as a function of Γ_s.

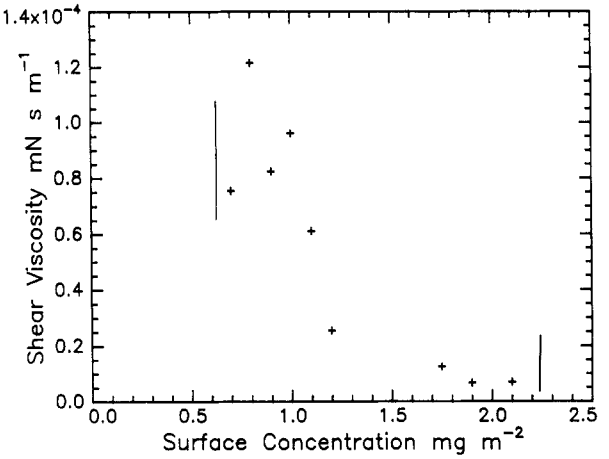

Figure 11. Transverse viscosity obtained by SQELS for synPMMA spread at the air–water interface.

Figure 6 are as predicted for a layer of uniform composition; hence, we conclude that the PMMA layer spread at the air–water interface has a uniform segment density. Consequently, $\rho_s(z)$ is a constant value over the region of the film thickness and zero at all other points, and the integral of dz in the definition of m given earlier is simply d, the layer thickness. Thus the scattering length density of the film, ρ_f, is m/d; values obtained by this means are quoted in Table II. The scattering length density of the film is the volume fraction weighted sum of all possible components of the film, i.e., polymer, air, and water.

$$\rho_f = \phi_p\rho_p + \phi_A\rho_A + \phi_w\rho_w \tag{11}$$

For the air contrast matched water both ρ_A and ρ_w are zero and the volume fraction of polymer in the film can be obtained directly using the scattering length density of the deuterated PMMA calculated from bound atom coherent scattering lengths (6.02×10^{-6} Å^{-2}). Table III reports the polymer volume fractions so obtained. Using the value of ρ_d obtained from the form factor plots, the volume fraction of water in the surface film of PMMA can be obtained in a similar fashion. If this is done, the volume fractions of water obtained are too large in that $(\phi_p + \phi_w) > 1$! However, the form factor plots obtained can be reproduced by four different scattering length density profiles[20] (Figure 13). Two of these have negative scattering length densities and are physically impossible; the two remaining models correspond to a film containing either a minor or major amount of a subphase (D_2O here), and the value of ρ_d given in Table II corresponds to the latter case. At the minimum in the form factor

$$Q^4R(Q)/(16\pi^2) = (2\rho_d - \Delta\rho)^2 \tag{12}$$

But

$$2\rho_d - \Delta\rho = 2\rho_d - (\rho_s - \rho_A)$$

Since ρ_A is zero, then

$$\begin{aligned} 2\rho_d - \Delta\rho &= 2\rho_d - \rho_s \\ &= 2(\rho_d - \rho_s) + \rho_s \\ &= -(2(\rho_s - \rho_d) - \Delta\rho) \end{aligned} \tag{13}$$

Thus on squaring the right-hand side of eq 13, it will be indistinguishable from the square of the left-hand side. Hence, the second scattering length density profile which would give the same Patterson plot is that with a minor component of water and corresponds to a scattering length density of $(6.35 \times 10^{-6} - \rho_d)$ Å^{-2} where 6.35×10^{-6} Å^{-2} is the scattering length density of bulk D_2O. This appears to be the situation prevailing here, since the values of ϕ_p obtained from Guinier plots are large. Calculating the volume fraction of water in the film using this second model (minor component of water) produces the values of ϕ_w given in Table III, and the variation of ϕ_p and ϕ_w with Γ_s is shown in Figure 14. These values and the shape of the form factors confirm the description that was concluded from the optical matrix analysis; i.e., the syndiotactic polymer forms a uniform layer at the air–water interface with a negligible fraction of the polymer immersed in the aqueous phase. As the surface film is compressed, the

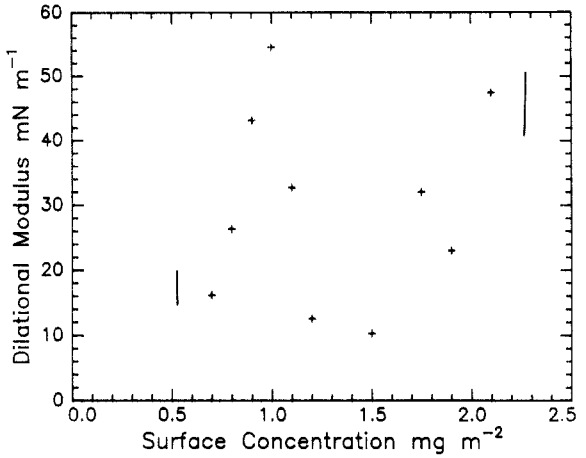

Figure 12. Surface layer dilational modulus obtained by SQELS for synPMMA spread at the air–water interface.

Table III
Volume Fraction Composition of Spread Films of Syndiotactic Poly(methyl methacrylate)

Γ_s/mg m^{-2}	ϕ_p	ϕ_w	ϕ_A[a]
0.3	0.17 ± 0.04		
0.4	0.21 ± 0.04	0.08_7 ± 0.03	0.7 ± 0.05
0.5	0.27 ± 0.03		
0.6	0.33 ± 0.03	0.08_9 ± 0.03	0.59 ± 0.04
0.8	0.58 ± 0.02	0.07 ± 0.03	0.35 ± 0.04
1.0	0.67 ± 0.02	0.09 ± 0.03	0.25 ± 0.04
1.5	0.90 ± 0.02	0.06 ± 0.03	0.04_2 ± 0.04
2.0	0.95 ± 0.02	0.07 ± 0.03	0

[a] Obtained by the difference $\phi_A = 1 - (\phi_p + \phi_w)$.

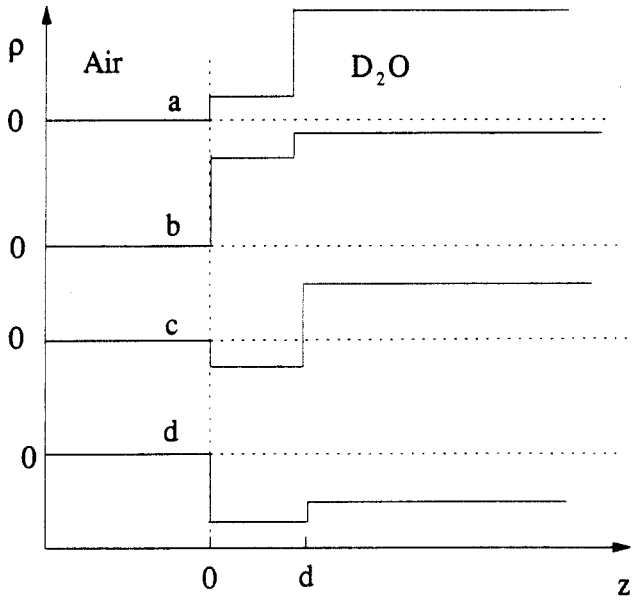

Figure 13. Possible scattering length density profiles which would all produce the form factor plots shown in Figure 5. Only a and b are physically realistic for hydrogenous synPMMA spread on D_2O; c and d have negative scattering length densities in part or in total.

water and air are "squeezed" out of the polymer film, which becomes almost totally composed of polymer. The major benefit of this elementary application of the kinematic approximation is that it is much easier to apply than the optical matrix method. However, it should be noted that the accuracy of the value of ρ_d obtained using eq 12 depends on a clear observation of the minimum and an accurate subtraction of the background. In addition to these simple applications of the kinematic approximation, eq 1 can be used to a much greater effect by use of partial structure

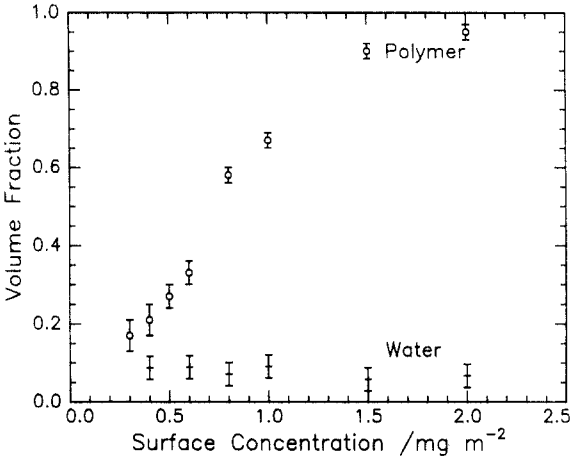

Figure 14. Volume fractions of polymer and water in a synPMMA film at the air–water interface obtained from neutron reflectometry data.

factors.[32] In real space, the scattering length density distribution normal to the polymer layer surface is

$$\rho(z) = \sum b_i n_i(z) \tag{14}$$

where b_i is the scattering length of species i and $n_i(z)$ the number density distribution of the same species. For a PMMA surface film containing water, eq 14 becomes

$$\rho(z) = b_p n_p(z) + b_w n_w(z) \tag{15}$$

On Fourier transforming and replacing in eq 1

$$R(Q) = (16\pi^2/Q^2)(b_p{}^2 h_{pp}(Q) + b_w{}^2 h_{ww}(Q) + 2b_p b_w h_{pw}(Q)) \tag{16}$$

with the subscripts p and w pertaining to polymer and water, respectively, and h_{ij} are the partial structure factors describing the correlation of species i with species j. For $i = j$, then $h_{ii}(Q) = |n_i(Q)|^2$, and for $i \neq j$, $h_{ij}(Q) = Re\, n_i(Q)\, n_j^*(Q)|$. Writing reflectivities in the form shown by eq 16 provides a very powerful insight into the structure of surface layers. This type of analysis has been pioneered by Thomas and co-workers[32,33] and applied to surfactants. A proper use of eq 16 requires $R(Q)$ to be measured with three differing contrast values. Under some circumstances or with the aid of certain assumptions, eq 16 may be simplified. For example on air contrast matched water

$$R(Q) = (16\pi^2/Q^2)(b_p{}^2 h_{pp}(Q))$$

and the partial structure factor can be obtained directly. If the PMMA layer is uniform and of thickness d

$$n_i(Q) = (2n_{ip}/Q)\sin(Qd/2)$$

where n_{ip} is the number density of segments of PMMA in the layer; hence

$$h_{pp}(Q) = (4n_{ip}{}^2/Q^2)\sin^2(Qd/2) \tag{17}$$

Figure 15 shows the fit of eq 17 to the data for PMMA at a surface concentration of 1.5 mg m^{-2}; note that data are actually plotted as $Q^2 h_{pp}(Q)$ as a function of Q. The fit obtained is reasonable, and from the values of n_{ip} and d obtained, the surface concentration is given by

$$\Gamma_s = n_{ip} d/\text{molecules Å}^{-2}$$

Values of n_{ip}, d, and Γ_s (converted to mg m^{-2}) obtained from this fitting procedure are given in Table IV. The agreement between the values of d in Tables II and IV is excellent. In general, the surface concentration calculated from a fit to the partial structure factor is larger than the

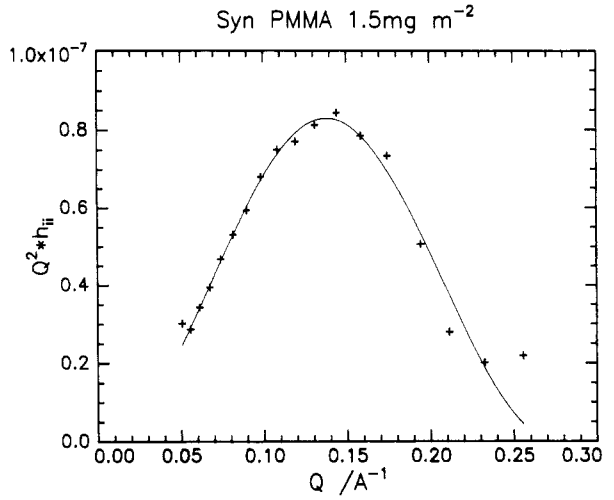

Figure 15. Fit of the uniform layer model (eq 17) to partial structure factor data for methyl methacrylate self-correlation.

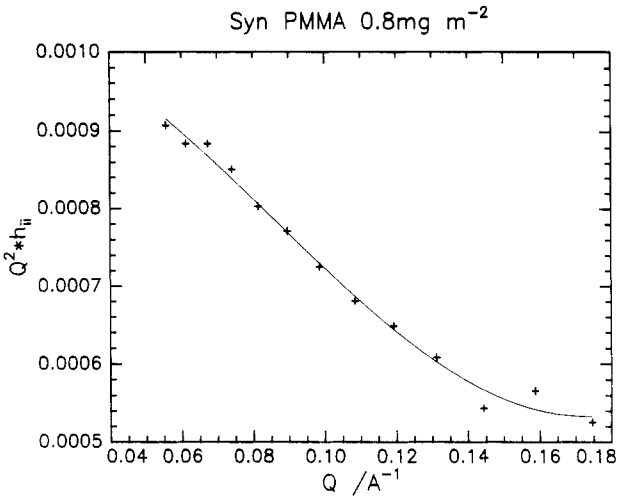

Figure 16. Fit of the uniform layer model (eq 18) to the partial structure factor of water in the surface film.

Table IV
Parameters of Uniform Layer Models from Fits to Partial Structure Factors

Γ_s/ mg m^{-2}	$n_{ip}/10^{-3}$ molecules Å^{-3}	d/Å	Γ_{calc}/ mg m^{-2}	$n_{w0}^2/10^{-3}$ molecules Å^{-6}	$n_{w1}/10^{-3}$ molecules Å^{-3}	t/Å
0.2				1.05	1.01	21.2
0.3	1.01	21.8	0.39			
0.4	1.09	21.7	0.42	1.04	1.01	18.8
0.5	1.59	20.5	0.58			
0.6	2.39	16.2	0.69	1.02	0.99	17.0
0.8	3.50	17.5	1.10	1.03	1.04	18.1
1.0	4.07	17.6	1.28	0.97	0.97	15.0
1.5	4.55	22.7	1.86	1.04	1.07	19.4
2.0	4.58	21.8	1.80	0.99	0.98	16.3

experimental value, but this parameter is extremely sensitive to the background subtraction and the discrepancies observed may be attributable to variations in the acuracy of this subtraction.

If the water, due to the presence of the polymer monolayer, also forms a uniform surface layer whose composition differs from that of the bulk water, then

$$h_{ww}(Q) = Q^{-2}(n_{w0}{}^2 + 4n_{w1}(n_{w1} - n_{w0}) \sin^2 (Qt/2)) \quad (18)$$

where n_{w0} is the bulk number density of the subphase, n_{w1} the surface layer number density, and t the thickness of the layer. For hydrogenous PMMA spread on D_2O, the scattering length of the polymer is very small, and if we assume it is essentially zero, then eq 16 becomes

$$R(Q) = (16\pi^2/Q^2)b_w{}^2 h_{ww}(Q)$$

At $Q = 0$, i.e., $z = \infty$, then $n_{w0}{}^2 = 1.099 \times 10^{-2}$ Å^{-6} for D_2O; in view of our assumption above, i.e., $b_p \approx 0$, then from fits to the data we expect $n_{w0}{}^2$ to be slightly less if the assumption is reasonably valid. At higher Q, the value of $Q^2h_{ww}(Q)$ should decrease. This behavior is seen in Figure 16 where a typical fit is displayed; the values of $n_{w0}{}^2$, n_{w1}, and t obtained are given in Table IV. The value of $n_{w0}{}^2$ is marginally less than that calculated from the bulk density and given above. However, the value of n_{w1} is much smaller than the bulk density and, together with the fact that the layer thickness of water is almost identical with that for the PMMA, then we presume this is strong evidence for a uniform distribution of water throughout the polymer surface film. However, what we cannot decide from the neutron reflectometry is whether the synPMMA is a continuous layer on the water surface or a series of "islands" separated from each other. The coherence length of the neutron beam incident on the surface is ca. 10^5 Å; consequently, any islands would have to have dimensions much greater than this length before any influence on the reflectometry profiles could be noted.

The surface tension data obtained by SQELS appear to be anomalous at low values of Γ_s in that they are higher than the accepted value for clean water! Given that the reproducibility of the values of γ_0 is excellent, one would perhaps suspect that either the apparatus was incorrectly aligned (i.e., a false value of Q was used) or the data fitting procedure was biased in some way. The counter to these arguments is that the SQELS analysis of pure water produced values of surface tension in excellent agreement with the accepted value.[19] The surface pressure isotherms are obtained by inserting the Wilhelmy slide into the water subphase and setting the readout to 0 mN m^{-1} for the clean water surface. It was noted that when synPMMA was spread onto the water surface from a chloroform solution, the surface pressure registered became negative and remained negative no matter what time was allowed for evaporation of solvent. An apparent increase of surface tension seems to have taken place. This observation now seems to be confirmed by the SQELS data, but the nature and source of this phenomenon is unclear and evidently further SQELS data are required for lower values of Γ_s. It appears to be intimately associated with the stereochemical nature of the polymer which has stronger intermolecular cohesive forces with itself rather than with the water subphase. This also seems to increase the cohesion of the water, thus increasing the surface tension. No such behavior is observed with isotactic poly(methyl methacrylate). Evidently, lower values of Γ_s need to be investigated, but the high values of γ_0 obtained do not seem to be an artifact of the techniques used. Figure 12 showed the variation in dilational modulus obtained from SQELS; the static dilational modulus ($\Gamma_s(d\pi/d\Gamma_s)$) obtained by a numerical differentiation of the surface pressure data has exactly the same shape and maximum value (Figure 17) as that obtained by SQELS, except that the static values are displaced to a higher value of Γ_s. This effect is also observable, although not to such a marked degree, in monolayers of low molecular weight materials.[19] The influence of the capillary wave frequency on the value of ϵ_0 should be to increase the value measured over that obtained by the static method. This increase is certainly observed at low values of Γ_s, where the static value is essentially zero. At higher values of Γ_s, the SQELS values are somewhat lower, but the scatter in the static values of the dilational modulus is such that firm conclusions cannot be made. Further information on whether the shift in the

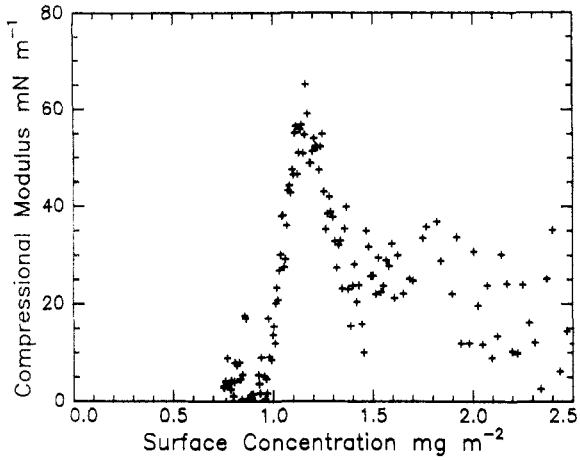

Figure 17. Surface layer dilational modulus obtained by numerical differentiation of the surface pressure isotherm of synPMMA spread at the air–water interface.

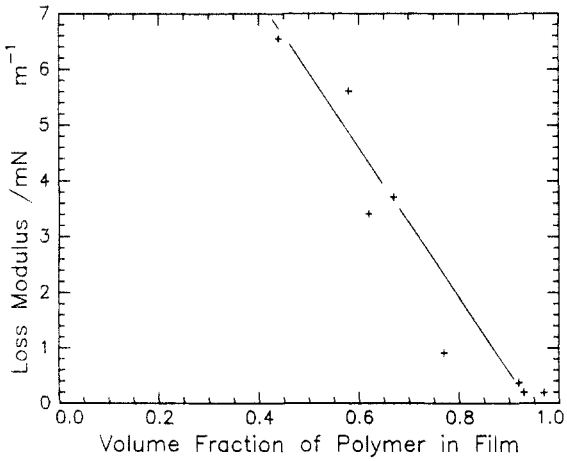

Figure 18. Loss modulus ($\omega\gamma'$) obtained from SQELS data for a synPMMA film as a function of the volume fraction of polymer in the film.

location of the maximum in ϵ_0 is frequency dependent requires SQELS measurements to be made at other frequencies, i.e., at different Q values. Unfortunately, as Q increases, the accuracy of the determination of ϵ_0 by SQELS decreases.

Similarly, the shear viscosity, γ', also goes through a maximum at almost the same value of Γ_s where the maximum in ϵ_0 is observed. It should be noted that the values of γ' are large, and therefore the accuracy of the values obtained may be questionable; however, as γ_0 decreases, the accuracy of the measurement of γ' increases. Nonetheless, the behavior observed is the same as that for spread films of low molecular weight spread films, i.e., a gradual increase in γ' as Γ_s decreases, followed by a rapid descent to zero after going through a maximum. Taking the analogy with viscoelastic phenomena further, we can identify the transverse storage modulus with γ_0 and the transverse loss modulus with $\omega_0\gamma'$.[34] This latter quantity appears to be linear in $1/\phi_p$ in the region we have investigated (Figure 18), but it must go through a maximum and decay rapidly at lower values of ϕ_p in order that a value of zero is obtained at $\Gamma_s = 0$.

Conclusions

The application of the kinematic approximation and contrast variation has allowed the structure of the surface layer structure of syndiotactic poly(methyl methacrylate) spread at the air–water interface to be determined. A combination of Patterson function analysis and Guinier analysis gives values for layer thickness and composition consistent with that is obtainable by optical matrix methods. The description provided is that of a coherent layer of polymer on the surface of the aqueous subphase with little interpenetration of water and polymer. Initially the content of the air in the film is high, but this rapidly decreases. The presence of air may indicate the existence of islands of polymer floating on the surface, but the coherence length of the neutron beam is too large to be sensitive to such islands; furthermore, the duration of a measurement is such that some temporal averaging takes place. The evaluation of the partial structure factors for methyl methacrylate units and water in the surface film confirms this view. The greater insight provided by this latter analysis should prove a powerful method of obtaining surface layer structures of many materials in the future. Attempts have been made to correlate this surface composition with the viscoelastic properties of the spread film measured by surface quasi-elastic light scattering. There is evidence for anomalous surface tension behavior at low surface coverages which warrants further investigation. The dilational modulus obtained by light scattering is of the same order of magnitude as that obtained from surface pressure data but is shifted to lower values of surface coverage. Transverse loss moduli calculated from the transverse shear viscosity appear to be approximately linearly related to the reciprocal of the surface film composition as determined from neutron reflectometry data in the range investigated here, but these data serve to reinforce the need to investigate very much lower surface concentrations where it appears changes in surface viscoelastic parameters take place most rapidly.

Acknowledgment. J.A.H. thanks the SERC for the provision of a maintenance grant during the course of this work. R.W.R. thanks the SERC for partial funding of the research project. J.A.H. and R.W.R. take great pleasure in thanking Professor John Earnshaw for his advice and encouragement with the SQELS experiments. All the authors acknowledge the vision of the SERC in providing and maintaining the pulsed neutron source, ISIS, at the Rutherford–Appleton Laboratory.

References and Notes

(1) Crisp, D. J. *J. Colloid Sci.* **1946**, *1*, 49.
(2) Crisp, D. J. *J. Colloid Sci.* **1946**, *1*, 161.
(3) Beredijk, N. *Newer Methods of Polymer Synthesis and Characterization*; Ke, B., Ed.; Wiley: New York, 1964.
(4) Shuler, R. L.; Zisman, W. A. *J. Phys. Chem.* **1970**, *74*, 1523.
(5) Ober, R.; Vilanove, R. *Colloid Polym. Sci.* **1977**, *255*, 1067.
(6) Vilanove, R.; Rondelez, F. *Phys. Rev. Lett.* **1980**, *45*, 1502.
(7) Takahashi, A.; Yoshida, A.; Kawaguchi, M. *Macromolecules* **1982**, *15*, 1196.
(8) Kawaguchi, M.; Yoshida, A.; Takahashi, A. *Macromolecules* **1983**, *16*, 956.
(9) Poupinet, D.; Vilanove, R.; Rondelez, F. *Macromolecules* **1989**, *22*, 2491.
(10) Brinkhuis, R. H. G.; Schouten, A. J. *Macromolecules* **1991**, *24*, 1496.
(11) Penfold, J.; Thomas, R. K. *J. Phys.: Condens. Matter* **1990**, *2*, 1369.
(12) Earnshaw, J. C. Laser Light Scattering. In *Polymer Surfaces and Interfaces*; Feast, W. J., Munro, H. S., Richards, R. W., Eds.; Wiley: London, 1992; to be published.
(13) Crowley, T. L.; Lee, E. M.; Simester, E. A.; Thomas, R. K.; Penfold, J.; Rennie, A. R. *Colloids Surf.* **1990**, *52*, 85.
(14) Langevin, D.; Meunier, J.; Chatenay, D. *Surfactants in Solution*; Mittal, K. L., Lindman, B., Eds.; Plenum: New York, 1984; Vol. 3.
(15) Earnshaw, J. C.; McGivern, R. C.; Crawford, G. E. *Dynamic Properties of Bimolecular Assemblies*; Harding, S. E., Rowe, A. J., Eds.; Royal Society of Chemistry: Cambridge, U.K., 1989.
(16) Henderson, J. A.; Richards, R. W.; Penfold, J.; Shackleton, C.; Thomas, R. K. *Polymer* **1991**, *32*, 3284.

(17) Kawaguchi, M.; Sauer, B. B.; Yu, H. *Macromolecules* **1989**, *22*, 1735.
(18) Langevin, D. *J. Colloid Interface Sci.* **1981**, *80*, 412.
(19) Earnshaw, J. C.; McGivern, R. C.; Winch, P. J. *J. Phys. Fr.* **1988**, *49*, 1271.
(20) Crowley, T. L.; Lee, E. M.; Simister, E. A.; Thomas, R. K. *Physica B* **1991**, *B173*, 143.
(21) Earnshaw, J. C. *Thin Solid Films* **1983**, *99*, 189.
(22) Earnshaw, J. C.; McGivern, R. C.; McLaughlin, A. C.; Winch, P. J. *Langmuir* **1990**, *6*, 649.
(23) The scattering length density is defined as $\sum b_i \rho N_A/m$, with b_i the bound atom coherent scattering length of atom i, ρ the physical density, m the molecular weight of the reflecting species, and N_A Avogadro's number.
(24) Strictly, the correlation function of $\rho(z)$ is called the Patterson function. However, it has also been used to describe the correlation function of the *gradient* in $\rho(z)$ as used here. See: Schlossman, M. L.; Pershan, P. S. In *Light Scattering by Liquid Surfaces and Complementary Techniques*; Langevin, D., Ed.; Marcel Dekker: New York, 1992; Chapter 18. Reference 20.
(25) Earnshaw, J. C.; McGivern, R. C. *J. Appl. Phys.* **1987**, *20*, 82.
(26) Bouchiat, M. A.; Meunier, J. *J. Phys. (Paris)* **1971**, *32*, 561.
(27) Levich, V. G. *Physicochemical Hydrodynamics*; Prentice-Hall: Englewood Cliffs, NJ, 1962.
(28) Gaines, G. L. *Insoluble Monolayers at Liquid–Gas Interfaces*; Wiley: New York, 1966.
(29) Byrne, D.; Earnshaw, J. *J. Colloid Interface Sci.* **1980**, *74*, 467.
(30) Hård, A.; Neuman, R. D. *J. Colloid Interface Sci.* **1981**, *83*, 315.
(31) Penfold, J. *Physica B* **1991**, *173*, 1.
(32) Simister, E. A.; Lee, E. M.; Thomas, R. K.; Penfold, J. *J. Phys. Chem.*, to be published.
(33) Lu, J. R.; Simister, E. A.; Thomas, R. K.; Rennie, A. R.; Penfold, J. *Langmuir*, to be published.
(34) Ferry, J. D. *Viscoelastic Properties of Polymers*, 2nd ed.; Wiley: New York, 1980.